

Homoharringtonine exhibits potent anti-tumor effect and modulates DNA epigenome in acute myeloid leukemia by targeting SP1/TET1/5hmC

Chenyang Li,^{1,2,3,*} Lei Dong,^{2,3,*} Rui Su,^{2,3,*} Ying Bi,⁴ Ying Qing,^{2,3} Xiaolan Deng,^{2,3,5} Yile Zhou,¹ Chao Hu,¹ Mengxia Yu,¹ Hao Huang,⁶ Xi Jiang,^{2,3,7} Xia Li,¹ Xiao He,¹ Dongling Zou,^{2,3,8} Chao Shen,^{2,3} Li Han,^{2,5} Miao Sun,⁹ Jennifer Skibbe,² Kyle Ferchen,² Xi Qin,^{2,3} Hengyou Weng,^{2,3} Huilin Huang,^{2,3} Chunxiao Song,⁴ Jianjun Chen^{2,3} and Jie Jin¹

¹Department of Hematology, The First Affiliated Hospital, Zhejiang University College of Medicine, Hangzhou, China; Key Laboratory of Hematologic Malignancies, Diagnosis and Treatment, Zhejiang, China; ²Department of Systems Biology & the Gehr Family Center for Leukemia Research, Beckman Research Institute of City of Hope, Monrovia, CA, USA; ³Department of Cancer Biology, University of Cincinnati, Cincinnati, OH, USA; ⁴Ludwig Institute for Cancer Research & Target Discovery Institute, Nuffield Department of Medicine, University of Oxford, Oxford, UK; ⁵School of Pharmacy, China Medical University, Shenyang, Liaoning, China; ⁶Division of Gynecologic Oncology, Feinberg School of Medicine, Northwestern University, Chicago, IL, USA; ⁷Department of Pharmacology, and Bone Marrow Transplantation Center of the First Affiliated Hospital, Zhejiang University School of Medicine; Institute of Hematology, Zhejiang University & Zhejiang Engineering Laboratory for Stem Cell and Immunotherapy, Hangzhou, Zhejiang, China; ⁸Department of Gynecologic Oncology, Chongqing University Cancer Hospital & Chongqing Cancer Institute & Chongqing Cancer Hospital, Chongqing, China; ⁹Department of Pediatrics, University of Cincinnati College of Medicine; Division of Human Genetics, Cincinnati Children's Hospital Medical Center, Cincinnati, OH, USA

*CL, LD and RS contributed equally to this work.

©2020 Ferrata Storti Foundation. This is an open-access paper. doi:10.3324/haematol.2018.208835

Received: October 8, 2018.

Accepted: April 9, 2019.

Pre-published: April 11, 2019.

Correspondence: JIE JIN - jiej0503@zju.edu.cn

JIANJUN CHEN - jianchen@coh.org

Supplementary Information

Homoharringtonine (HHT) exhibits potent anti-tumor effect and modulates DNA epigenome in acute myeloid leukemia by targeting SP1/TET1/5hmC

Chenyong Li, Lei Dong, Rui Su, Ying Bi, Ying Qing, Xiaolan Deng, Yile Zhou, Chao Hu, Mengxia Yu, Hao Huang, Xi Jiang, Xia Li, Xiao He, Dongling Zou, Chao Shen, Li Han, Miao Sun, Jennifer Skibbe, Kyle Ferchen, Xi Qin, Hengyou Weng, Huilin Huang, Chunxiao Song, Jianjun Chen, Jie Jin

I Methods and Materials (Pages 2-7)

II Supplemental Figures (Pages 8-15)

III Supplemental Tables (Pages 16-21)

METHODS AND MATERIALS

Cell proliferation, cell apoptosis, and cell cycle assay

Cells were seeded in 96-well plates at the concentration of 5,000-10,000 cells per well in triplicates and MTT (G4000, Promega) was used to assess cell growth/proliferation. For cell apoptosis assay, PE Annexin V Apoptosis Detection Kit I (BD Pharmingen) were applied according to the manufacturer's instructions. For cell cycle assay, Propidium iodide (PI) DNA staining was employed and cells were resuspended in Krishan's reagent (0.05mg/ml PI, 0.1% trisodium citrate, 0.02mg/ml ribonuclease A, 0.3% NP-40), incubated at 37°C for 30 minutes and then applied to the flow cytometer.

Cell differentiation assay

ATRA- or PMA-induced myeloid differentiation of human AML cells are described in detail as follows. Two classic myeloid differentiation cell model were applied in this paper. For the PMA-induced monocytic differentiation model, MONOMAC 6 cells were pretreated with HHT at different concentrations (10 and 20 ng/ml, PBS as control) for 24 hours, and then PMA (10 nM as final concentration) was added to the medium. After 48 and 96 hours, cells were collected and analyzed by flow cytometry and qPCR. CD11b, CD14 and CSF1R were applied as monocytic marker. For the ATRA-induced granulocytic differentiation model, NB4 cells were pretreated with HHT at different concentrations (5 and 10 ng/ml, PBS as control) for 24 hours, and then ATRA (1 μ M as final concentration) was added to the medium. After 48 and 96 hours, cells were collected and analyzed by flow cytometry and qPCR. CD11b, CD15 and CSF3R were applied as granulocytic marker

Similarly, both monocytic differentiation and granulocytic differentiation of human CD34+ cord blood cells were conducted in this paper. The CD34+ cord blood cells were cultured in SFEM medium supplemented with L-glutamine and lipid mixture. To induce monocytic differentiation, the following human cytokines were added into the medium, 2 ng/ml IL-3, 100 ng/ml SCF, 50 ng/ml M-CSF, 1 ng/ml IL-6 and 100 ng/ml Flt3-ligand. CD11b and CD14 were used as monocytic marker to confirm the successful induction. To induce granulocytic differentiation, the following human cytokines were added into the medium, 2 ng/ml IL-3, 100 ng/ml SCF, 20 ng/ml G-CSF and 10 ng/ml IL-6. Every 3 days, medium was refreshed and samples were collected.

Flow cytometry analysis

All the samples were performed on a LSR Fortessa flow cytometer (BD Bioscience) and analyzed with FlowJo software (Tree Star Inc., Ashland, OR). Flow cytometry analyses of mouse cells were conducted as described previously with some modifications.^{1,2} The following antibodies were used for staining cells, APC-conjugated anti-human CD45 (17-9459-42, eBioscience), APC-conjugated anti-human CD33 (12-0339-42), PE-conjugated anti-mouse CD45.2 (12-0454-82), PE-conjugated anti-human CD11b (12-4714-81), APC-conjugated anti-human CD14 (17-0149-42), APC-conjugated anti-human CD15 (17-0158-41).

Colony forming assay

Leukemic bone marrow(BM) blast cells collected from primary BMT recipient mice carrying MLL-AF9- or NRAS+AE9a (*AML1-ETO9a* fusion gene plus *NRAS^{G12D}*)-induced full-blown AML were seeded into methylcellulose medium dishes (with 10,000 cells per dish), supplied with murine recombinant IL-3, IL-6, GM-CSF, and SCF (10 ng/ml for the first three and 30 ng/ml for SCF; R&D Systems, Minneapolis, MN), along with PBS or HHT(5ng/ml or 10ng/ml) . Cells were incubated at 37°C with 5% CO₂ under humid atmosphere for 7 days. Then, colony cells were collected and plated in methylcellulose dishes every 7 days with 10,000 cells/dish for 3 passages. Colony numbers and cell counts were evaluated for each passage.

RNA extraction, qPCR assay and RNA-seq analysis

MA9.3ITD and MA9.3RAS cells were treated with PBS or HHT (5ng/ml or 10ng/ml) for 48 hours before collected and total RNA was collected by use of the miRNeasy Mini Kit (Qiagen). qPCR was conducted with 2× SYBR Master Mix (Thermo Fisher) in the AB 7900HT Fast Real-Time PCR system (Applied Biosystem) with specific primers (supplemental table 1) in triplicates.

For RNA-sequencing analysis, NEB (New England Biolabs) Next Ultra Directional RNA Library Prep Kit were applied to prepare libraries. PrepX mRNA Library kit (WaferGen) combined Apollo 324 NGS automated library prep system was also used. Libraries at the final concentration of 15 pM were clustered onto a single read (SR) flow cell using Illumina TruSeq SR Cluster kit v3, and sequenced to 50 bp using TruSeq SBS kit on Illumina HiSeq system. Differential gene expressions

were analyzed by standard Illumina sequence analysis pipeline. The Gene Set Enrichment Analysis (GSEA)³ was used to analyze the enriched signaling pathway in PBS or HHT treated cell samples.

DNA extraction and dot blot

MA9.3ITD and MA9.3RAS cells were treated with PBS or HHT (5ng/ml or 10ng/ml) for 48 hours before collected and their DNA samples were then extracted with DNeasy Blood & Tissue Kit (69506, Qiagen). For DNA dot blot assay, the samples were added to 0.1N NaOH, denatured at 99°C for 5 minutes, neutralized by adding 0.1 volume of 6.6M ammonium acetate, and loaded on Hybond-N+ membrane (GE Healthcare). After UV crosslinking, the membrane was stained with 0.02% methylene blue (Sigma-Aldrich), washed with PBST buffer, blocked with 5% milk, and then incubated with 5mC antibody (39649, Active Motif) or 5hmC antibody (39769, Active Motif) overnight at 4°C. Then the membrane was incubated with HRP-conjugated goat anti-rabbit IgG (Santa Cruz Biotechnology) for 1 hour at room temperature and then developed with Pierce™ ECL Western Blotting Substrate (Thermo Fisher).

For 5hmC sequencing, genomic DNA was fragmented and 5hmC was labelled with 6-N3-glucose using β -GT enzyme. Biotin tags were added onto the 6-N3-glucose with Huisgen cycloaddition (click) chemistry reaction using DBCO-PEG4-biotin. The biotin-labelled 5hmC containing DNA was enriched with streptavidin-coupled magnetic beads. The enriched DNA was used for library preparation and next-generation sequencing.⁴

Protein extraction and Western blotting

Proteins were extracted with RIPA buffer (Sigma-Aldrich) containing protease inhibitor and phosphatase inhibitor cocktail (78420, Thermo Fisher). The protein concentration was determined with BCA protein assay kit (23225, Thermo Fisher). An estimated 30-60 μ g protein was loaded per well on 6-10% SDS-PAGE gel and transferred onto PVDF membrane (Thermo Fisher) pre-activated by methanol. Membranes were washed with PBST, blocked with 5% milk and incubated with antibodies against SP1 (ab13370, Abcam), TET1 (A-1020-050, Epigentek), FLT3 (3462, Cell Signaling Technology), MYC (ab32072, Abcam), HOXA9 (ab140631, Abcam), MEIS1 (ab19867, Abcam), GAPDH (sc-47724, Santa Cruz Biotechnology Inc.), and β -Actin (3700S, Cell Signaling Technology). Secondary antibodies and detection were according to routine laboratory practices.

Nuclear run-on assay

Nuclear run-on reactions were performed by supplying biotin-16-UTP to nuclei, thus labeled transcripts were bound to streptavidin-coated magnetic beads as reported before with minor modifications.^{5, 6} MA9.3ITD cells treated with PBS or HHT for 48 hours were harvested and resuspended in Nonidet P-40 lysis buffer (10 mM Tris-Cl, pH 7.4, 10 mM NaCl, 3 mM MgCl₂, and 0.5% NP-40). Each nuclear pellet was resuspended in 396 μ l nuclear freezing buffer (50 mM Tris-HCl, pH 8.3, 40% glycerol, 5 mM MgCl₂, and 0.1 mM EDTA). 100 μ l of 5 \times run-on buffer (25 mM Tris-Cl, pH 8.0, 750 mM KCl, 12.5 mM MgCl₂, 1.25 mM each of ATP, GTP and CTP) was added in the nuclei along with 4 μ l biotin-16-UTP (11388908910, Sigma-Aldrich) for run-on reaction. After incubation at 29°C for 30 min, the reaction was terminated by the addition of 0.75 μ l 1M CaCl₂, and 3 μ l RNase-free DNase I and incubated at 29°C for another 10 minutes. RNA purification was performed with RNeasy mini kit (74104, Qiagen) according to the manufacturer's protocol. A small aliquot (5 μ l from a total of 50 μ l) was saved as “total nuclear RNA” for each sample. Dynabeads M-280 streptavidin (11205D, Thermo Fisher Scientific) were mixed with an equal volume of the isolated RNA samples at 42°C for 20 minutes and at room temperature for 2 hours. After washing with 2 \times SSC, the beads were resuspended in 25 μ l of nuclease-free water. Reverse transcription PCR and qPCR were performed as mentioned before. The PCR products were then applied for the 2% agarose gel analysis and photos were taken by Gel DocTM XR System (BIO-RAD).

Drug affinity responsive targets stability (DARTS)

To identify whether SP1 is a direct target of HHT, DARTS was conducted following the published protocol.^{7, 8} Briefly, 30 \times 10⁶ MA9.3ITD cells were lysed in M-PER (78501, Thermo Fisher Scientific) lysis buffer. Then TNC buffer was added and the protein concentration was determined by BCA assay. Cell lysates were then incubated with varying concentrations of HHT or PBS for 1 hour and digested with Pronase (1:10000) for 30 minutes at room temperature. The digestion was stopped by protease inhibitor cocktail and the samples were immediately added with SDS loading buffer and heated. Subsequently, Western blotting was conducted and GAPDH was used as a negative control.

Cellular Thermal Shift Assay (CETSA)

To determine the direct binding between HHT and SP1 in cellular, CETSA was performed according to the published protocol.⁹ Briefly, 20×10^6 MA9.3ITD cells were pretreated with 5ng/ml HHT for 12 hours and then chilled on ice, washed once and then transferred into 200 ml PCR tubes. Cells were heat shocked with the Thermal Cycler at gradient temperatures for 3 minutes to denature proteins, and immediately cooled down at room temperature for 3 minutes. Finally, all the samples were applied to three freeze-thaw cycles to lyse cells, and centrifuged at 20,000 g for 20 minutes at 4°C to pellet cell debris with aggregated proteins. The supernatant was boiled with 4x Laemmli Sample Buffer and then subjected to western blot. The bands were quantified using Gel-Pro analyzer software and plotted with three biological replicates.

Lentivirus and retroviral production, precipitation and infection

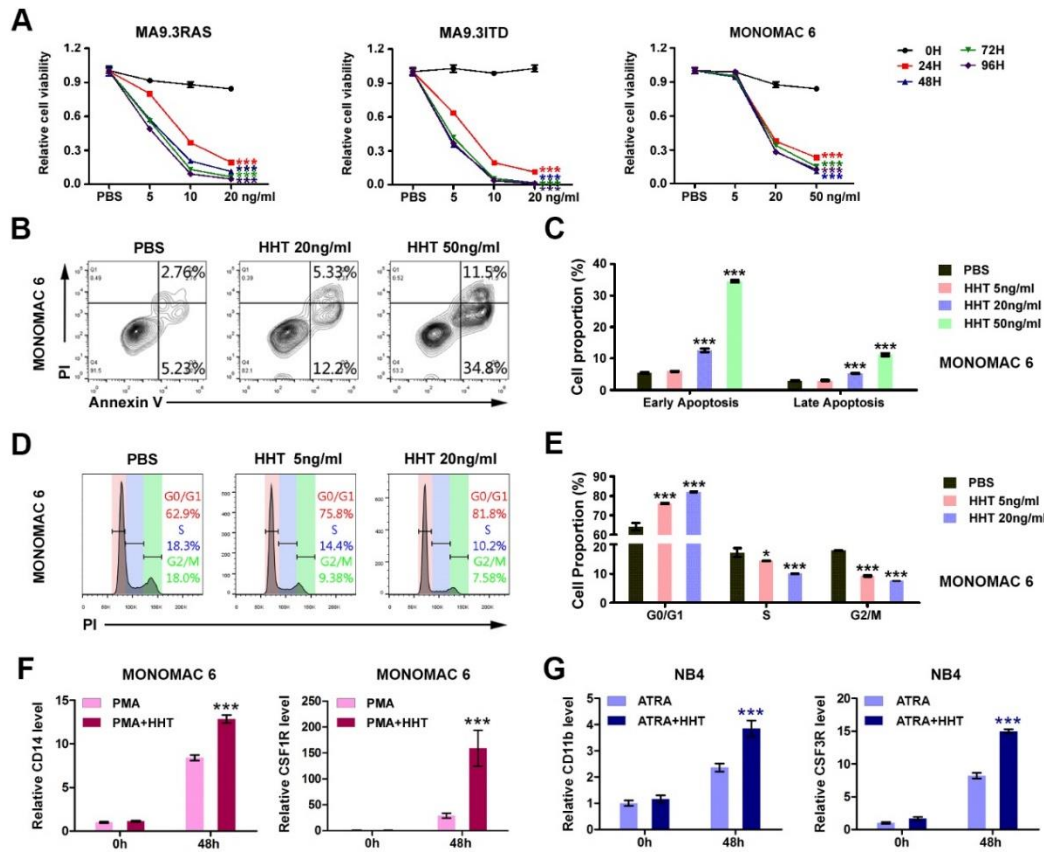
Human small hairpin RNAs (shRNAs) including shTET1-A, shTET1-C, shSP1-D, shSP1-E and shNS with the lentiviral vector (PLKO.1) were purchased from Dharmacon and packaged with third generation lentivirus package system as reported before.¹⁰ Mouse *Tet1* shRNAs including shTet1a, shTet1b and shTET1a+b with a retroviral vector (pGFP-V-RS) were constructed and packaged as reported before.¹¹ Human FLT3 overexpression plasmids including FLT3 WT, FLT3 ITD and empty vector T2A were kindly offered by Dr. Ling Li and packaged with second generation lentivirus package system as reported before.² The medium containing virus particles were harvested at 48 and 72 hours and concentrated with PEG-it virus precipitation solution (LV810A-1, SBI). For infection, add the virus particle directly into cells with existence of 4 µg/ml polybrene (H9268, Sigma-Aldrich). The positive infected cells were selected with specific markers. For the high titer FLT3 or FLT3-ITD virus, supernatant (20 ml) was concentrated ~200× and was used for one time infection.

Chromatin immunoprecipitation (ChIP) assay

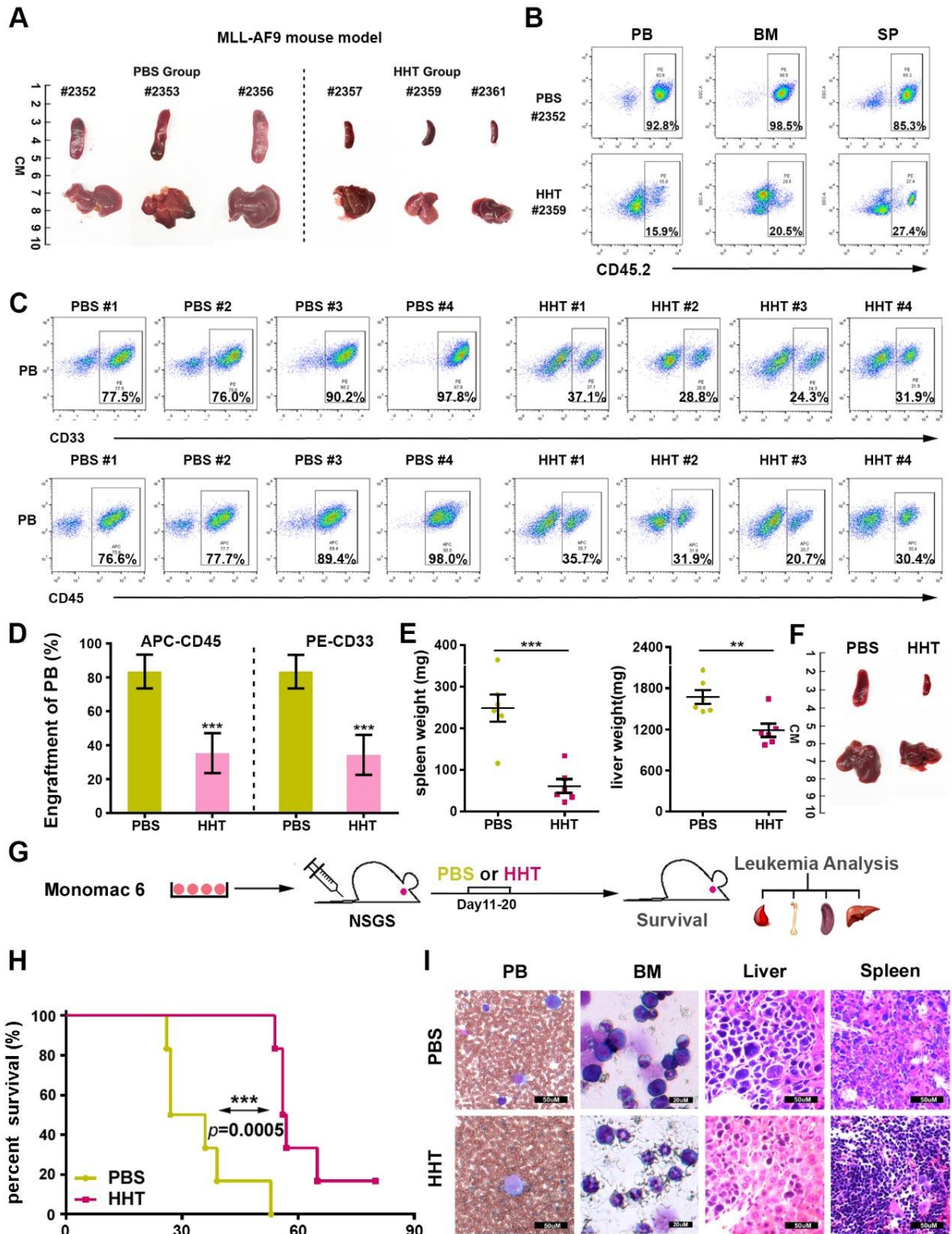
ChIP assay was performed with EpiTech ChIP One Day Kit (334471, Qiagen) following the manufacturer's protocol, with some modifications. Briefly, MA9.3ITD cells or MONOMAC 6 cells were treated with 1% formaldehyde for 10 min at 37 °C to crosslink DNA and proteins. The reaction was terminated by the addition of stop buffer and incubated at room temperature for 5 minutes. After cell lysis, the cross-linked chromatin was sonicated to an average size of ~500 bp

(Bioruptor Pico Sonication System). The antibodies against SP1 (ab13370, Abcam), 5hmC, TET1, MLL (Abcam, Cambridge, MA), H3K79me2, or IgG (Millipore) was used for immunoprecipitation. Purified ChIP DNA was amplified by qPCR using specific primers (supplemental Table 2) targeting the SP1 binding site on the promoter region of *TET1* and the 5hmC peaks on *FLT3*.

Supplemental Figures



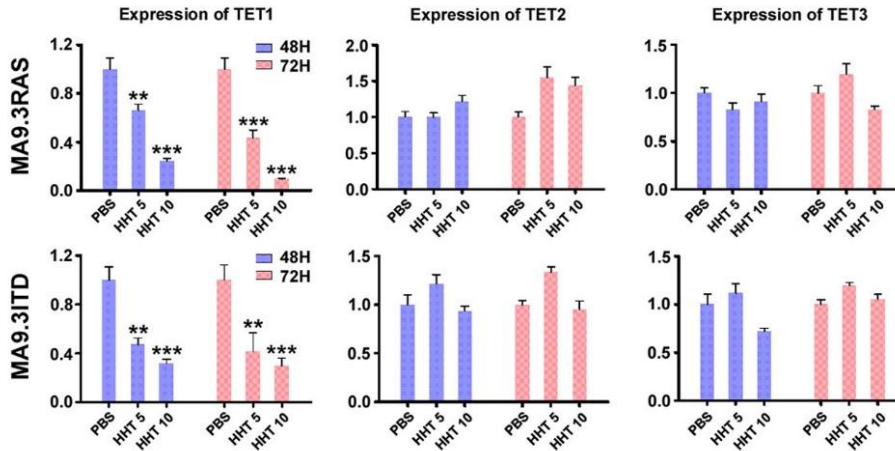
Supplemental Figure 1. AML cells display high sensitivity to HHT treatment *in vitro*. (A) Effects of HHT treatment on cell viability in MA9.3RAS, MA9.3ITD and MONOMAC 6 at different time points (0, 24, 48, 72 and 96 hours). (B) Effects of HHT on apoptosis in MONOMAC 6 cells. Cells were treated with HHT (0, 5, 20, 50 ng/ml; or, 0, 9.2, 36.7, 91.64 nM) for 48 hours and representative flow cytometric plots and percentages of cell apoptosis are shown. (C) Statistical apoptosis analysis from 3 independent experiments determined by flow cytometry. (D) Function of HHT on cell cycle arrest in MONOMAC 6 cells. Cells were treated with HHT for 48 hours and representative flow cytometric plots and percentages of cell cycle phases are shown. (E) Statistical cell cycle analysis from 3 independent experiments determined by flow cytometry. (F) Statistical q-PCR analysis of CD14 and CSF1R in MONOMAC 6 cells upon HHT treatment for 96 hours during PMA-induced monocytic differentiation. (G) Statistical q-PCR analysis of CD11b and CSF3R in NB4 cells upon HHT treatment for 96 hours during ATRA-induced granulocytic differentiation. *, $P < 0.05$; **, $P < 0.01$; ***, $P < 0.001$; t -test. Error bar, mean \pm SD.



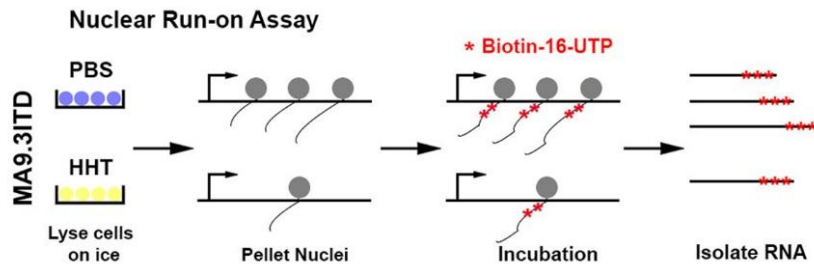
Supplemental Figure 2. HHT inhibits the progression of AML *in vivo*. (A) Representative images of spleens (SP) and livers at the end point of the PBS- or HHT-treated *MLL-AF9* mouse

model. (B) Staining of CD45.2 in peripheral blood (PB), bone marrow (BM) and spleen (SP) at the end point of *MLL-AF9* mice coupled with PBS or HHT treatment. (C) Staining of CD33 and CD45 in PB of the NSGS mice that were transplanted with human MA9.3ITD AML cells. (D) Statistical analysis of the engraftment ratio of the leukemic cells into PB of the recipient NSGS mice. (E) SP and liver weights in PBS- or HHT-treated NSGS mice xeno-transplanted with MA9.3ITD AML cells at their end points. (F) Representative images of SP and liver in PBS- or HHT-treated MA9.3ITD leukemic mice. (G) Schematic illustration of the MONOMAC 6 AML xenograft NSGS coupled with HHT or PBS treatment. (H) Kaplan-Meier curves of PBS or HHT-treated NSGS mice that were transplanted with human MONOMAC 6 AML cells. (I) Wright-Giemsa staining of mouse PB and BM, and hematoxylin and eosin (H&E) staining of liver and SP from PBS or HHT treated MONOMAC 6 leukemic mice. Bars represent 50 μ M for PB, SP and Liver; 20 μ M for BM. *, $P < 0.05$; **, $P < 0.01$; ***, $P < 0.001$; t -test. Error bar, mean \pm SD. For Kaplan-Meier curve, P values were calculated by log-rank test.

A



B



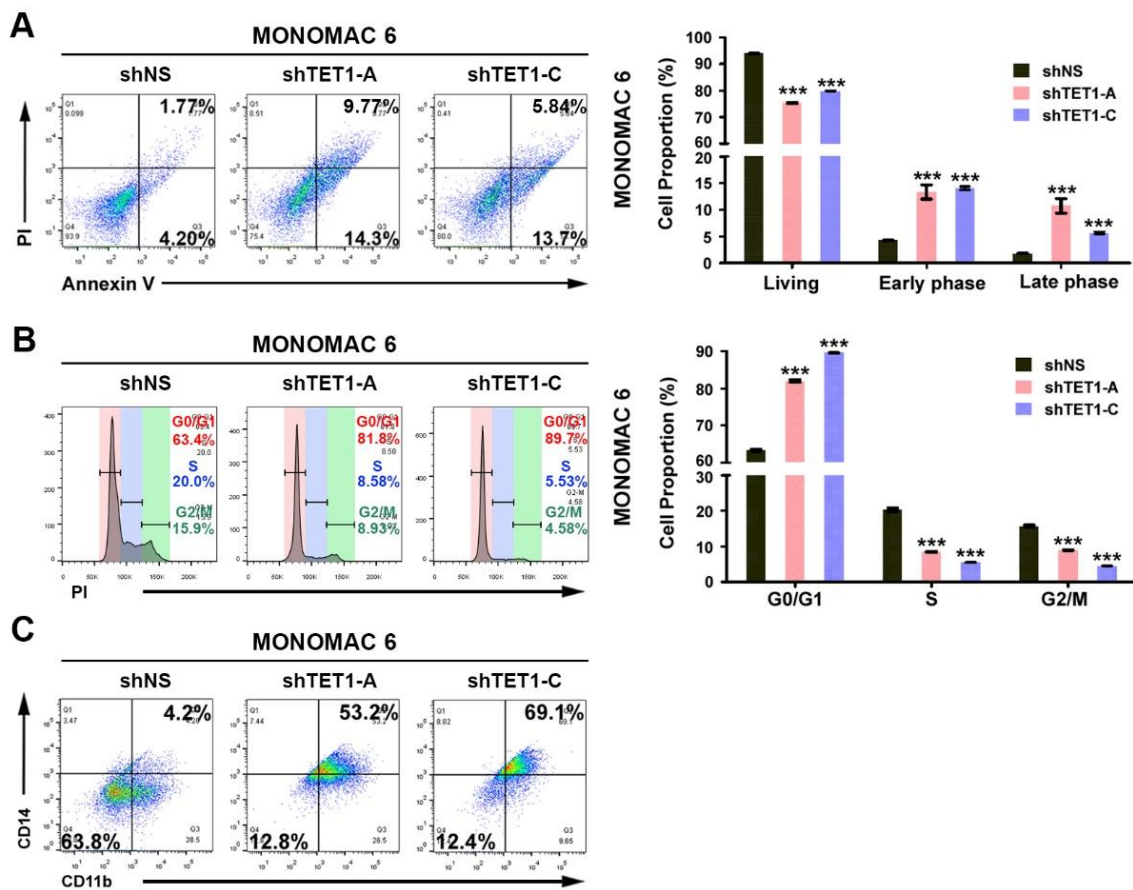
C

Corresponding Sp1 binding sites at ~500bp upstream of TET1 transcription start site

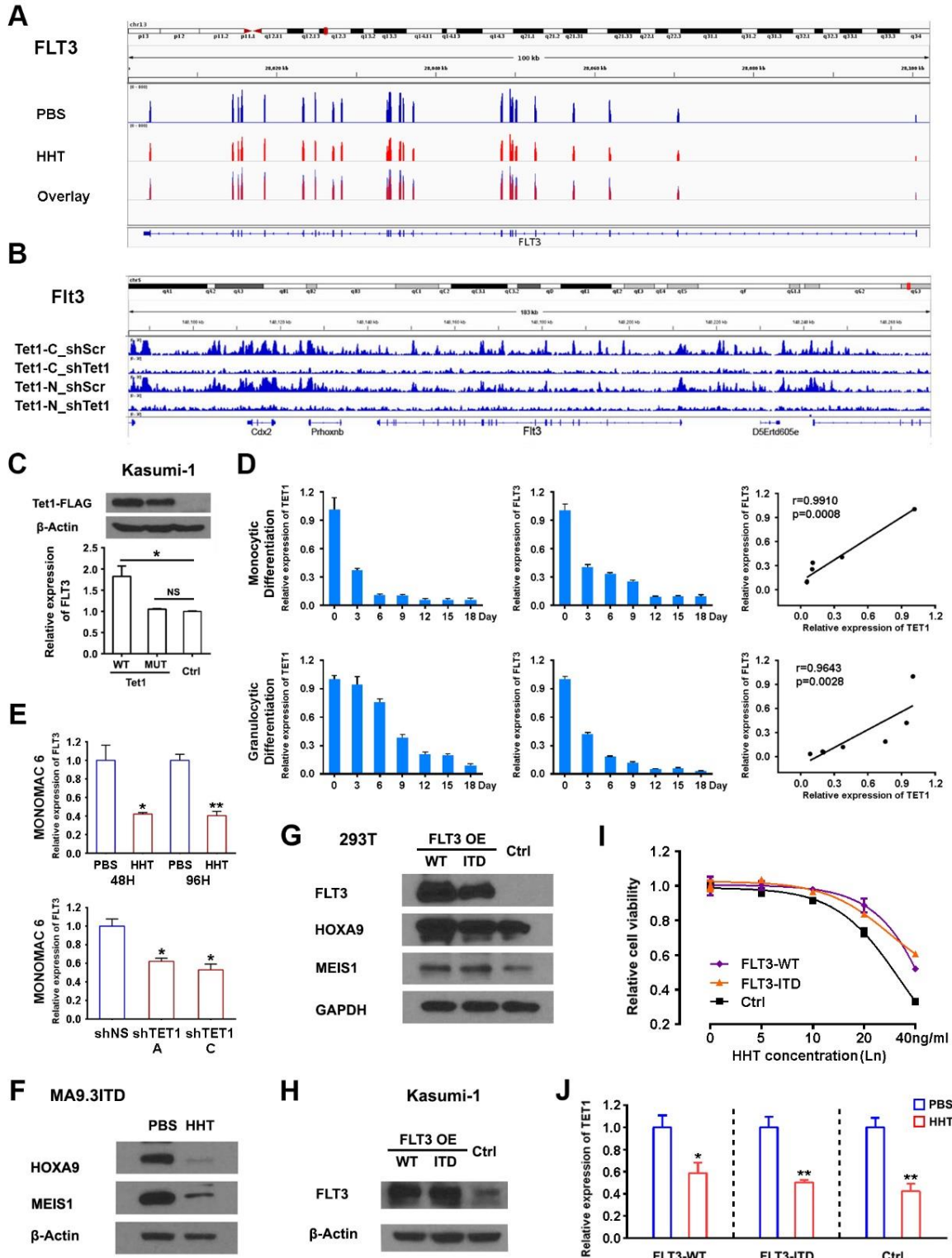
-530	CTAATTCGGA	AAACTT ^{Site 1} AGCT	CTTCCTGCC	TTTCATTTCT	TCATTCATAA	AGTGAATACG
-470	^{Site 2} ACCACCACTG	^{Site 3} AGGTCCAGGG	CCAAATAACT	AACAGAAATA	TTATGATGAA	CTTTCAGAC
-410	^{Site 4} ATCCAGCCCA	GAGTCAGGGA	ACACAGCCCT	CATCTGGTTT	CTCTCTTTGG	TGTT ^{Site 5} GAGGGC
-350	GGTTTTCCGT	TGCTGGCGAC	CTAGACATTG	CTCAATGGTG	TCATCTCTGA	CCTGGCACCT
-290	TCTTCATACA	TTTATAAACA	TGCAATTTAG	AGATCCTAAA	AACTTTTTCT	AGAGCTCCCC
-230	TGGGAAAAAA	GTTAATGACA	AAATCTTGAC	ACCTCTCTAC	GTCCTCT ^{Site 6} TCG	GAGACAGAGA
-170	AGTTGAG ^{Site 7} AGA	GGTGGAGAAC	GAGGGGGAGG	GGGAGGGGGT	CGAGAGGGAG	TC ^{Site 9} GAGGAGGG
-110	ATCCAGCTC	CAGTTTGGGT	AAATCCAGCT	CGCGTTTTGT	CTCTCGCTCA	ACTGTGCAGG
-50	GTCCAGCGAA	GGCAGAGCCC	CAGCTTCACT	CCCTGAGGTC	TGTCCTGGGG	AG ⁺¹ ACTGCT

TSS

Supplemental Figure 3. HHT substantially reduces global 5hmC abundance via targeting SP1/TET1 in AML. (A) Effects of HHT on expression of *TET1*, *TET2*, and *TET3* in AML cells upon 5 or 10 ng/ml HHT treatment for 48 or 72 hours. (B) Schematic illustration of nuclear run-on assay in MA9.3ITD cells treated with PBS or HHT (5 ng/ml) for 48 hours. Total RNA was prepared and biotinylated RNA was isolated using streptavidin magnetic beads (Run-on RNA). (C) The transcription factor binding sites were highlighted in yellow. The arrow denotes the start site of *TET1* transcription. **, $P < 0.01$; ***, $P < 0.001$; t -test. Error bar, mean \pm SD.

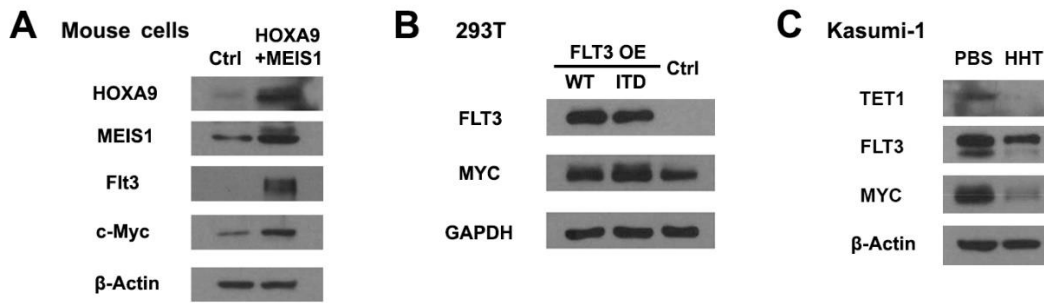


Supplemental Figure 4. Knockdown of *TET1* expression recapitulates phenotypes with HHT treatment in AML. (A) Effects of *TET1* knockdown on apoptosis in MONOMAC 6 cells, along with statistical analysis of apoptosis assay from 3 independent experiments determined by flow cytometry. (B) Effects of *TET1* knockdown on cell cycle arrest in MONOMAC 6 cells, and statistical analysis of cell cycle assays of 3 independent experiments determined by flow cytometry. (C) Effects of *TET1* knockdown on monocytic differentiation by staining with CD11b and CD14 in MONOMAC 6 cells. * $P < 0.05$; ** $P < 0.01$; *** $P < 0.001$; t -test. Error bar, mean \pm SD.



Supplemental Figure 5. FLT3 is a critical target of the HHT-TET1/5hmC axis. (A) The view of mRNA abundance across *FLT3* genomic locus in MA9.3ITD cells with PBS or HHT (10 ng/ml)

treatment. (B) The binding of Tet1 on *Flt3* genomic locus in control (shScr, scrambled shRNA) and Tet1 knockdown (shTet1) mouse ES cells with two different Tet1 antibodies (Tet1-C and Tet1-N, binding to the C-terminal and N-terminal of Tet1 respectively). (C) The relative expression of FLT3 in Tet1-WT or Tet1-Mut overexpressed Kasumi-1 cells, empty vector were applied as control. (D) Relative expression of *TET1* and *FLT3* during monocytic and granulocytic differentiation of cord blood derived CD34⁺ HSPCs (left and middle panel). The positive relation between *FLT3* and *TET1* during the differentiation are shown (right panel). (E) qPCR results of the relative expression of *FLT3* in HHT treated and *TET1* knockdown MONOMAC 6 cells. (F) Western blot analysis of HOXA9 and MEIS1 in HHT-treated MA9.3ITD. (G) Western blot analysis of FLT3, HOXA9 and MEIS1 in FLT3 or FLT3-ITD overexpressed 293T cells. (H) Western blot analysis to confirm the overexpression of FLT3 or FLT3-ITD in Kasumi-1 cells. (I) The sensitivity of Kasumi-1 cells with or without FLT3 overexpression to HHT treatment. The cells with treated with different concentrations of HHT for 24 hours. (J) qPCR analysis of the relative expression of *TET1* and *FLT3* in Kasumi-1 cells with FLT3 or FLT3-ITD overexpression after treated with HHT for 24 hours. *, $P < 0.05$; **, $P < 0.01$; ***, $P < 0.001$; *t*-test. Error bar, mean \pm SD.



Supplemental Figure 6. MYC signaling is a major downstream pathway affected by the HHT-SP1/TET1/5hmC axis. (A) Western blot analysis of HOXA9, MEIS1, Flt3 and c-myc in HOXA9/MEIS1 co-overexpressed mouse bone marrow cells. (B) Western blot analysis of FLT3 and MYC in FLT3 or FLT3-ITD overexpressed 293T cells. (C) Western blot analysis of TET1, FLT3 and MYC in HHT-treated Kasumi-1 cell.

Supplemental Table 1. Information of the primers used for quantitative RT-qPCR

Primer	Sequence
TET1 Forward	CAGAACCTAAACCACCCGTG
TET1 Reverse	TGCTTCGTAGCGCCATTGTAA
TET2 Forward	CCCTTCTCCGATGCTTTCT
TET2 Reverse	TGGGTTATGCTTGAGGTGTTT
TET3 Forward	AAGACACCTCGCAAGTTCC
TET3 Reverse	GTTGGTCACCTGGTTCTGATA
ACTB Forward	CACTCTTCCAGCCTTCCTC
ACTB Reverse	GTACAGGTCTTTGCGGATGT
FLT3 Forward	AGGGACAGTGTACGAAGCTG
FLT3 Reverse	GCTGTGCTTAAAGACCCAGAG

Supplemental Table 2. Information of the primers used for ChIP-qPCR

Primer	Sequence
FLT3 Forward-1	TGCTTAGCCTTTTCGCCACT
FLT3 Reverse-1	TTGATTCCATCCTCGTCCC
FLT3 Forward-2	TTTATCAGGACCAGGACAC
FLT3 Reverse-2	ACTTTCATGGCTTCATTTC
FLT3 Forward-3	CGTTCTCCAAGACCCTATC
FLT3 Reverse-3	CTCTTAACGCAGCCTTTCT
FLT3 Forward-4	GTTGAGATTTGGGTGGTGA
FLT3 Reverse-4	GGAAGGCATGATTGATTTT
FLT3 Forward-5	CAGGTTCAAGCGATTCTCC
FLT3 Reverse-5	TCAAGACCAGCCTAGCAAA
FLT3 Forward-6	CAGGAGGTTGAGGTAGGAG
FLT3 Reverse-6	CTTTAGCCTGGTCAGAAAA
SP1 Forward-1	TCTTAATTCTGGCGTAATGC
SP1Reverse-1	CAGTGGTGGTCGTATTCA
SP1 Forward-2	AATACGACCACCACTGAG
SP1Reverse-2	CAGAGATGACACCATTGAG
SP1 Forward-3	ACCTGGCACCTTCTTCAT
SP1Reverse-3	CTCTCAACTTCTCTGTCTCC
SP1 Forward-4	GGAGACAGAGAAGTTGAGAG
SP1Reverse-4	CACAGTTGAGCGAGAGAC

Supplementary Table 3. TOP 100 potential targets regulated by the HHT-TET1/5hmC axis, Related to Figure 5

	Target genes	P value	Chromosome	Strands
1	FAM69C	2.70E-06	chr18	-
2	CENPF	3.91E-06	chr1	+
3	FLT3	5.07E-06	chr13	-
4	MKI67	6.59E-06	chr10	-
5	TOP2A	8.61E-06	chr17	-
6	PAN3	1.01E-05	chr13	+
7	RASL11A	6.08E-05	chr13	+
8	JMJD1C	7.09E-05	chr10	-
9	ADPGK	7.60E-05	chr15	-
10	BAHCC1	8.32E-05	chr17	+
11	TCF4	1.01E-04	chr18	-
12	NCAPH	1.29E-04	chr2	+
13	CCNB2	1.29E-04	chr15	+
14	GNA13	1.32E-04	chr17	-
15	GAB2	1.42E-04	chr11	-
16	USP48	1.52E-04	chr1	-
17	MYCBP2	1.62E-04	chr13	-
18	BLM	1.73E-04	chr15	+
19	PKMYT1	1.76E-04	chr16	-
20	TEX2	1.77E-04	chr17	-
21	SLC38A10	2.13E-04	chr17	-
22	NUSAP1	2.14E-04	chr15	+
23	LIN9	2.22E-04	chr1	-
24	TUBB	2.28E-04	chr6	+
25	SPEN	2.38E-04	chr1	+
26	STMN1	2.46E-04	chr1	-
27	CDKN2C	2.80E-04	chr1	+
28	NEK2	2.95E-04	chr1	-
29	FUT4	2.99E-04	chr11	+
30	FAM105A	3.03E-04	chr5	+
31	NRM	3.03E-04	chr6	-
32	CIT	3.04E-04	chr12	-
33	TIFA	3.06E-04	chr4	-
34	PRC1	3.29E-04	chr15	-
35	GGA3	3.29E-04	chr17	-
36	NEK9	3.34E-04	chr14	-
37	MDC1	3.52E-04	chr6	-
38	ALDH1A3	3.60E-04	chr15	+
39	TUBGCP3	3.65E-04	chr13	-
40	PANK2	3.70E-04	chr20	+
41	GTSE1	3.90E-04	chr22	+

42	MIF4GD	3.95E-04	chr17	-
43	DNAJC10	4.00E-04	chr2	+
44	CDCA8	4.08E-04	chr1	+
45	TEX12	4.10E-04	chr11	+
46	ANLN	4.15E-04	chr7	+
47	AXIN1	4.16E-04	chr16	-
48	C1orf106	4.18E-04	chr1	+
49	MRPS12	4.21E-04	chr19	+
50	SARS2	4.26E-04	chr19	-
51	E2F8	4.33E-04	chr11	-
52	MFSD11	4.41E-04	chr17	+
53	FAM83D	4.56E-04	chr20	+
54	ACOT7	4.62E-04	chr1	-
55	CMPK2	4.79E-04	chr2	-
56	HMGB2	4.86E-04	chr4	-
57	SLC9A3R1	4.87E-04	chr17	+
58	SP2	5.12E-04	chr17	+
59	MCM8	5.31E-04	chr20	+
60	CDCA7	5.31E-04	chr2	+
61	SENP8	5.32E-04	chr15	+
62	OIP5	5.42E-04	chr15	-
63	MRPL28	5.47E-04	chr16	-
64	AK2	5.73E-04	chr1	-
65	LIG3	5.83E-04	chr17	+
66	SIRT7	5.98E-04	chr17	-
67	TK1	6.03E-04	chr17	-
68	ZDHHC13	6.03E-04	chr11	+
69	PIF1	6.11E-04	chr15	-
70	CEP350	6.13E-04	chr1	+
71	VRK1	6.18E-04	chr14	+
72	LYST	6.18E-04	chr1	-
73	PKD1	6.32E-04	chr16	-
74	POLA2	6.32E-04	chr11	+
75	PRR11	6.36E-04	chr17	+
76	POLE2	6.69E-04	chr14	-
77	PAPD5	6.79E-04	chr16	+
78	IL12B	6.90E-04	chr5	-
79	NUP210	6.95E-04	chr3	-
80	TMEM109	6.98E-04	chr11	+
81	CDC6	7.00E-04	chr17	+
82	REEP4	7.04E-04	chr8	-
83	CDC20	7.44E-04	chr1	+
84	TMED8	7.50E-04	chr14	-
85	CDCA2	7.62E-04	chr8	+
86	AXL	7.65E-04	chr19	+
87	SORBS3	7.69E-04	chr8	+

88	TMEM123	7.75E-04	chr11	-
89	IQGAP3	7.78E-04	chr1	-
90	ARHGAP11A	7.79E-04	chr15	+
91	TSEN54	7.96E-04	chr17	+
92	TMEM104	8.06E-04	chr17	+
93	H2AFZ	8.18E-04	chr4	-
94	NPLOC4	8.31E-04	chr17	-
95	SMC4	8.31E-04	chr3	+
96	TRAIP	8.51E-04	chr3	-
97	ETV6	8.51E-04	chr12	+
98	CARS2	8.61E-04	chr13	-
99	HIRIP3	8.71E-04	chr16	-
100	LRRFIP1	8.77E-04	chr2	+

Supplemental Table 4. Information of the AML patients used in the functional studies

Patient ID	FAB subtype	Molecular genetics	Cytogenetic
AML#1	M4 De novo	FLT3-ITD Pos., NPM1 Neg., CEBPA Neg., C-Kit Neg., IDH1 Neg., IDH2 Neg.	Normal
AML#2	M1 De novo	FLT3-ITD Pos., NPM1 Pos., CEBPA Pos., C- Kit Neg., IDH1 Neg., IDH2 Neg.	Normal
AML#3	M4 De novo	FLT3-ITD Pos., NPM1 Pos., CEBPA Neg., C- Kit Neg., IDH1 Neg., IDH2 Neg.	Normal
AML#4	M2a Relapsed/refractory	FLT3-ITD Pos., NPM1 Neg., CEBPA Neg., C-Kit Neg., IDH1 Neg., IDH2 Neg.	Normal

References

1. Jiang X, Huang H, Li Z, et al. Blockade of miR-150 maturation by MLL-fusion/MYC/LIN-28 is required for MLL-associated leukemia. *Cancer Cell*. 2012;22(4):524-535.
2. Su R, Dong L, Li C, et al. R-2HG Exhibits Anti-tumor Activity by Targeting FTO/m(6)A/MYC/CEBPA Signaling. *Cell*. 2018;172(1-2):90-105 e123.
3. Subramanian A, Tamayo P, Mootha VK, et al. Gene set enrichment analysis: a knowledge-based approach for interpreting genome-wide expression profiles. *Proc Natl Acad Sci U S A*. 2005;102(43):15545-15550.
4. Song CX, Szulwach KE, Fu Y, et al. Selective chemical labeling reveals the genome-wide distribution of 5-hydroxymethylcytosine. *Nat Biotechnol*. 2011;29(1):68-72.
5. Smale ST. Nuclear run-on assay. *Cold Spring Harb Protoc*. 2009;2009(11):pdb prot5329.
6. Lee YL, Chiao CH, Hsu MT. Transcription of muscle actin genes by a nuclear form of mitochondrial RNA polymerase. *PLoS One*. 2011;6(7):e22583.
7. Lomenick B, Olsen RW, Huang J. Identification of direct protein targets of small molecules. *ACS Chem Biol*. 2011;6(1):34-46.
8. Lomenick B, Jung G, Wohlschlegel JA, Huang J. Target identification using drug affinity responsive target stability (DARTS). *Current protocols in chemical biology*. 2011;3(4):163-180.
9. Jafari R, Almqvist H, Axelsson H, et al. The cellular thermal shift assay for evaluating drug target interactions in cells. *Nat Protoc*. 2014;9(9):2100-2122.
10. Li Z, Weng H, Su R, et al. FTO Plays an Oncogenic Role in Acute Myeloid Leukemia as a N6-Methyladenosine RNA Demethylase. *Cancer Cell*. 2017;31(1):127-141.
11. Huang H, Jiang X, Li Z, et al. TET1 plays an essential oncogenic role in MLL-rearranged leukemia. *Proc Natl Acad Sci U S A*. 2013;110(29):11994-11999.